Canadian Journal of Pure and Applied Sciences
Vol. 9, No. 2, pp. 3409-3422, June 2015
Online ISSN: 1920-3853; Print ISSN: 1715-9997
Available online at www.cjpas.net

INHIBITION EFFECT OF PHENYLAMINE ON THE CORROSION OF AUSTENITIC STAINLESS STEEL TYPE 304 IN DILUTE SULPHURIC ACID

*Roland Tolulope Loto[1,2], Cleophas Akintoye Loto[1,2] and Abimbola Patricia Popoola[2]
[1]Department of Mechanical Engineering, Covenant University, Ota, Ogun State, Nigeria
[2]Department of Chemical, Metallurgical and Materials Engineering,
Tshwane University of Technology, Pretoria, South Africa

ABSTRACT

The corrosion of austenitic stainless steel (type 304) in dilute sulphuric acid solutions in addition to recrystalized sodium chloride concentrates in the presence of specific proportions of phenylamine was studied with the aid of polarization resistance technique, electrode potential monitoring and coupon method. Results showed the overwhelming influence of the compound in corrosion inhibition with an inhibition efficiency of 97.5% from coupon analysis and 86.10% from polarization test at highest observed concentration of the inhibitor. Corrosion potential measurement showed potentials well with passivation values. Corrosion rate decreased progressively with increase in concentration of phenylamine. The adsorption of the compound on the steel surface followed the Langmuir isotherm model. Thermodynamic variables of adsorption surmised showed the interaction mode with the steel to be physiochemical and spontaneous. Observation from scanning electron microscopy and x-ray diffractometry showed the electrochemical impact on the surface topography and the phase compounds of the steel samples studied. Results from statistical analysis depict the sharp influence of inhibitor concentration on the electrochemical performance of the compound.

Keywords: Aminobenzene, sulphuric acid, Langmuir, corrosion, inhibition.

INTRODUCTION

Millions of dollars are lost each year because of corrosion. Much of this loss is due to the corrosion of iron and steel although many other metals do corrode as well. Corrosion damage causes leakage of fluids or gases in devices and containers made of alloy materials. Even more dangerous is the loss of strength of engineering structures induced by corrosion leading to subsequent failure. Stainless steel type 304 is widely used in many applications such as desalination plants, construction materials, pharmaceutical industry, thermal power plant, chemical cleaning and pickling process, oil and gas industry etc, due to their stability, good corrosion resistance, high strength, workability and weldability (Selvakumar *et al*., 2013). Stainless steels resist corrosion through the formation of a thin oxide layer on the metal surface in aqueous acid environments. These films are usually thin, compact and enriched in chromium (Olsson and Landolt, 2000; Bera *et al*., 2000; Taveira *et al*., 2005; Deflorian and Rossi, 2006). However in highly corrosive environments the protective passive surface layer of the steel is destroyed resulting in corrosion of the stainless steel (Mieczyslaw and Joanna, 2013). Corrosion has a strong influence in the oil industry, due to the location of actual production formations in hostile environments. Acids are consistently pumped into wells to enhance productivity through increase in formation permeability (Negm and Mohamed, 2004; Martin, 2003; Kane, Negm and Aiad 2007; Bhaskaran *et al*., 2003; Wojtanowicz, 2008).

Use of chemical compounds is one of the most cost effective techniques for corrosion control in harsh industrial conditions (Trabenelli, 1991; Ferreira *et al*., 2004; Bouklah *et al*., 2006; Gopi *et al*., 2000; Hosseini *et al*., 2009; Akrout *et al*., 2007; Gopi *et al*., 2007). The compounds known as inhibitors are usually added in specific quantities in applications such as acid pickling of steel, petroleum industry, oil well acidizing, boiler plants etc., for corrosion prevention (Popova *et al*., 2003; Noor, 2005; Sk *et al*., 2003; Chetouani *et al*., 2004; Dadgarnezhad *et al*., 2004). The inhibitors form a protective impenetrable covering over the metallic surface through adsorption especially by chemisorptions mechanism. Adsorption depends majorly on the molecular configuration of the chemical inhibiting compound, the electrochemical characteristics of the corrosive media, the property of the alloy topography and the electrode potential of metal/solution boundary. This

*Corresponding author e-mail: tolu.loto@gmail.com

electrolytic mechanism is associated with physiochemical interaction on the alloy surface.

Interests in corrosion inhibition have majorly been directed to organic compounds (Bouklah *et al*., 2006; Obot *et al*., 2010; Satapathy *et al*., 2009). A significant number of researches have shown that organic compounds containing mainly nitrogen, sulphur or oxygen atoms in their structure to be effective inhibitors. The study aims to investigate the corrosion inhibition efficiency and adsorption mechanism of phenylamine on austenitic stainless steel (type 304) in 3 M sulphuric solution capable of destroying the passivity of the steel with the aid of weight loss test, potentiodynamic polarization and open circuit potential measurement. Scanning electron microscopy and X-ray diffractometry were applied to investigate the inhibition characteristics in the acid solution. The experimental results were analyzed through adsorption isotherms, corrosion thermodynamics and statistical analysis.

MATERIALS AND METHODS

Material

Austenitic stainless steel (type 304) used for this investigation has the following composition; 18.11 Cr, 8.32 Ni and 68.32% Fe. The steel has a cylindrical dimension of 18 mm diameter.

Inhibitor

Phenylamine (PNL) a brownish, translucent liquid obtained from SMM Instruments, South Africa is the inhibitor used. The structural formula of PNL is shown in figure 1. The molecular formula is $C_6 H_5 NH_2$ while the molar mass is 93.13 $gmol^{-1}$.

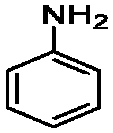

Fig. 1. Chemical structure of Phenylamine (PNL).

PNL was prepared in volumetric concentrations of 1.25%, 2.5%, 3.75%, 5%, 6.25% and 7.5% per 200ml of the acid solution.

Test Media

Sulphuric acid (analar grade) of 3M concentration with 0.6M sodium chloride (recrystallised) were employed as the corrosive media.

Metallographic analysis

The stainless steel rod was machined into a number of samples with average length from 17.8 and 18.8 mm. The surface of the samples were ground with Silicon carbide papers of 80, 120, 220, 800 and 1000 grits before being polished with 6 to 1 μm diamond paste. The samples were later washed with distilled water, rinsed with acetone, dried and stored in a dessicator for further test.

Weight-loss experiments

The test coupons were immersed in 200 ml of the acid solution at predetermined concentrations of the PNL for 360h at 25°C. The coupons were weight every 72 h after being washed with distilled water, rinsed with acetone and dried. Graphs of weight-loss (mg) and corrosion rate (mmpy) versus exposure time (h) (Figs. 2, 3) for the steel coupons and those of percentage inhibition efficiency (η) versus exposure time (h) and percentage PNL concentration (Figs. 4, 5) were made from table 1.

The corrosion rate (R) is calculated as shown below:

$$R \text{ (mmpy)} = \left[\frac{87.6W}{DAT}\right] \quad (1)$$

W (mg) is the weight loss, D (g/cm^3) is the density, A (cm^2) is the area and T (hrs) is the exposure time. The η was calculated from the equation.

$$\eta = \left[\frac{W1-W2}{W1}\right] \text{ x } 100 \quad (2)$$

W_1 and W_2 are the weight loss with and without the addition of PNL. The η was calculated for the inhibitor concentrations every 72 h. The surface coverage (θ) was calculated from

$$\theta = \left[1 - \frac{W2}{W1}\right] \quad (3)$$

Open circuit potential measurement

A two-electrode electrochemical cell with a silver/silver chloride was used as reference electrode. The measurements of OCP were obtained with Autolab PGSTAT 30 ECO CHIMIE potentiostat. Resin mounted test electrodes/specimens with exposed surface of 254 mm^2 were fully and separately immersed in 200 ml of the test solution at specific concentrations of PNL for a total of 288h. The potential of each of the test electrodes was measured every 48 h. Plots of potential (mV) versus immersion time (h) (Fig. 6) for the test media were made from the tabulated values in table 2.

Potentiodynamic polarization

Potentiodynamic polarization test were carried out with cylindrical steel samples mounted in resin plastic with a bare surface area of 254 mm^2. The samples were grinded with specific category of silicon carbide paper, polished to 1 μm, rinsed by distilled water and dried with acetone. The analysis were done at 25°C with Autolab PGSTAT 30 ECO CHIMIE potentiostat and electrode cell containing 200 ml of the acid solution, with and without

PNL. The counter electrode used is made of graphite and Ag/AgCl is the reference electrode. The steady state open circuit potential (OCP) was noted. The potential were cursorily exmined from -1.5V *vs* OCP to +1.5 mV *vs* OCP at a scan rate of 0.002 V/s. The corrosion current density (I_{cr}) and corrosion potential (E_{cr}) were calculated from the Tafel plots. The corrosion rate (R), the extent of surface coverage (θ) and the percentage inhibition efficiency (η) were calculated according to the equation;

$$R = \frac{0.00327 * I_{cr} * eq.wt}{D} \quad (4)$$

Where I_{cr} (μA/cm^2) is the current density in, D (g/cm^3) is the density, *eq.wt* (g) is the equivalent weight. The percentage inhibition efficiency (η) was calculated from the corrosion rate as follows;

$$\eta = 1 - \left[\frac{R_1}{R_2}\right] \times 100 \quad (5)$$

where R_1 and R_2 are the corrosion rates with and without PNL respectively.

Scanning electron microscopy characterization

The surface morphology of the uninhibited and inhibited stainless steel specimens was investigated after weight-loss analysis in 3 M H_2SO_4 solutions using Jeol scanning electron microscope for which SEM micrographs were recorded.

X-Ray diffraction analysis

X-ray diffractometry (XRD of the film formed on the metal surface without PNL addition was done using a Bruker AXS D2 phaser desktop powder diffractometer with monochromatic Cu Kα radiation produced at 30 kV and 10 mA, with a step size of 0.03° 2θ. The Measurement program is the general scan xcelerator. Analysis of the steel sample inhibited with PNL was done with PANalytical X'Pert Pro powder diffractometer with X'Celerator detector and variable divergence- and receiving slits with Fe filtered Co-Kα radiation. The phases were identified using X'Pert Highscore plus software.

Statistical Analysis

Two-factor single level statistical analysis using ANOVA test (F-test) was performed so as to investigate the

Table 1. Data obtained from weight loss measurements for austenitic stainless steel in 3 M H_2SO_4 in the presence of specific concentrations of the PNL at 360h.

Sample	Weight Loss (g)	Corrosion Rate (mm/yr)	Molarity (C)	Inhibitor Concentration (%)	Inhibition Efficiency (%)	Surface Coverage (θ)
A	2.401	11.85	0	0	0	0
B	0.958	3.92	0.00027	2.5	60.1	0.6010
C	0.144	0.46	0.00054	5	94.002	0.9400
D	0.241	1.03	0.00081	7.5	89.963	0.8996
E	0.111	0.47	0.00107	10	95.377	0.9538
F	0.110	0.54	0.00134	12.5	95.419	0.9542
G	0.058	0.21	0.00161	15	97.584	0.9758

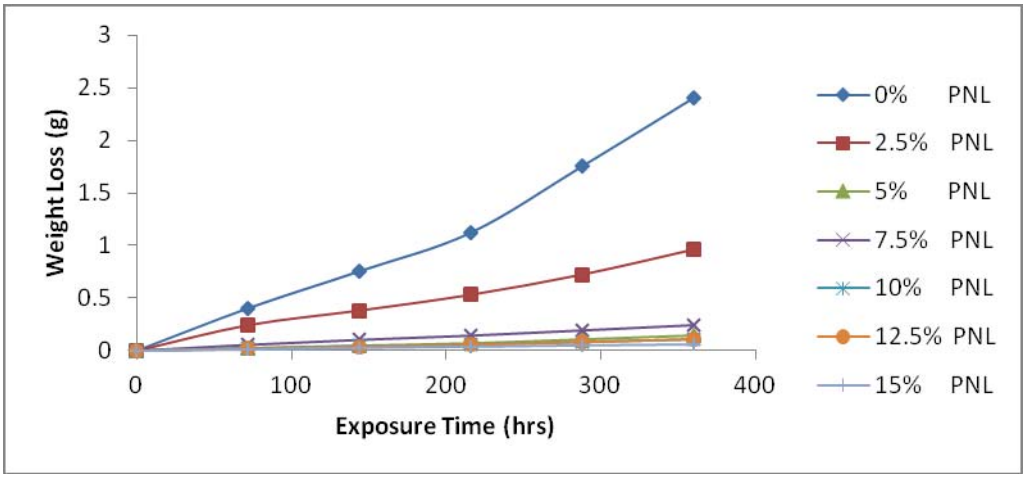

Fig. 2. Variation of weight-loss with exposure time for samples (A – G) in 3 M H_2SO_4

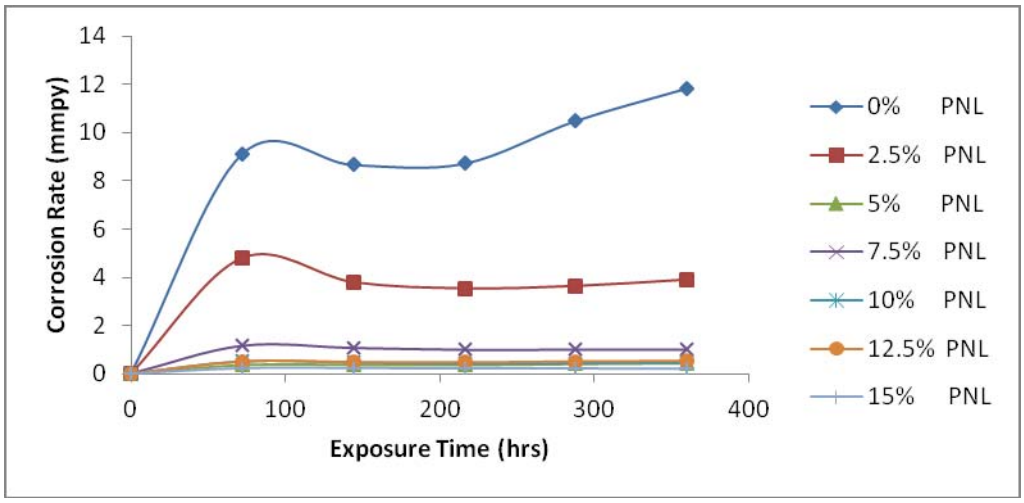

Fig. 3. Effect of percentage concentration of PNL on the corrosion rate of austenitic stainless steel in 3 M H_2SO_4

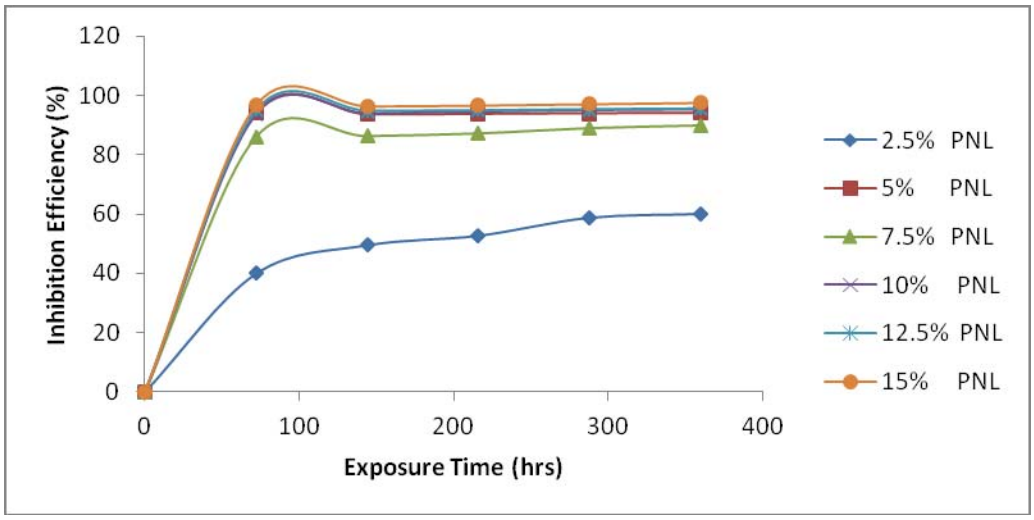

Fig. 4. Plot of inhibition efficiencies of sample (A-G) in 3 M H_2SO_4 during the exposure period

significant effect of inhibitor concentration and exposure time on the inhibition efficiency values of PNL in the acid media.

RESULTS AND DISCUSSION

Weight-loss measurements

Weight-loss of austenitic stainless steel at various time intervals, in the absence and presence of PNL concentrations in 3 M H_2SO_4 acid at 25°C was studied. The values of weight-loss (W), corrosion rate (R) and the percentage inhibition efficiency (η) are presented in table 1.Decrease in corrosion rate is due to increase in concentration of PNL due to availability of more PNL molecules for corrosion inhibition adsorption on the alloy surface. This is responsible for increase in surface coverage of the alloy specimen. Figures 2, 3 and 4 show the relationship between weight-loss, corrosion rate and percentage inhibition efficiency with exposure time at exact PNL concentration while figure 5 shows the relationship between η and PNL concentration. The plots derived show progressive increase in η with increase in PNL concentration accompanied by a significant decrease in corrosion rate.

Open Circuit Potential Measurement

The open-circuit potential values of the of the stainless steel specimens was observed for a total of 288h in the sulphuric acid solution in the absence and presence of specific concentrations of PNL inhibitor. The results are shown in table 2 and figure 6, respectively. In the test solutions a progressive potential displacement towards negative values was noticed in 0% PNL concentrations during the immersion hours. This corresponds with anodic dissolution of the steel specimen in the absence of PNL.

At 1.25% PNL concentration there is a gradual positive shift in corrosion potential to the noble direction due to

Table 2. Data obtained from potential measurements for austenitic stainless steel in 3 M H_2SO_4 in presence of specific concentrations of the PNL.

PNL Concentration (%) / Exposure Time (h)	0	1.25	2.5	3.75	5	6.25	7.5
0	-358	-460	-328	-331	-324	-307	-294
48	-341	-446	-316	-319	-325	-318	-297
96	-361	-373	-305	-328	-312	-318	-297
144	-364	-387	-312	-325	-300	-315	-301
192	-365	-356	-306	-313	-295	-311	-299
240	-430	-321	-299	-304	-298	-308	-300
288	-444	-334	-301	-297	-301	-305	-297

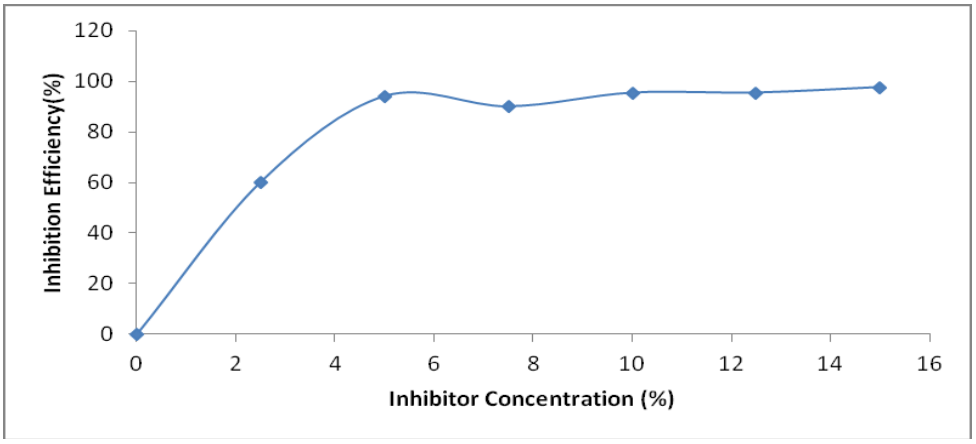

Fig. 5. Variation of percentage inhibition efficiency of PNL with inhibitor concentration in 3 M H_2SO_4

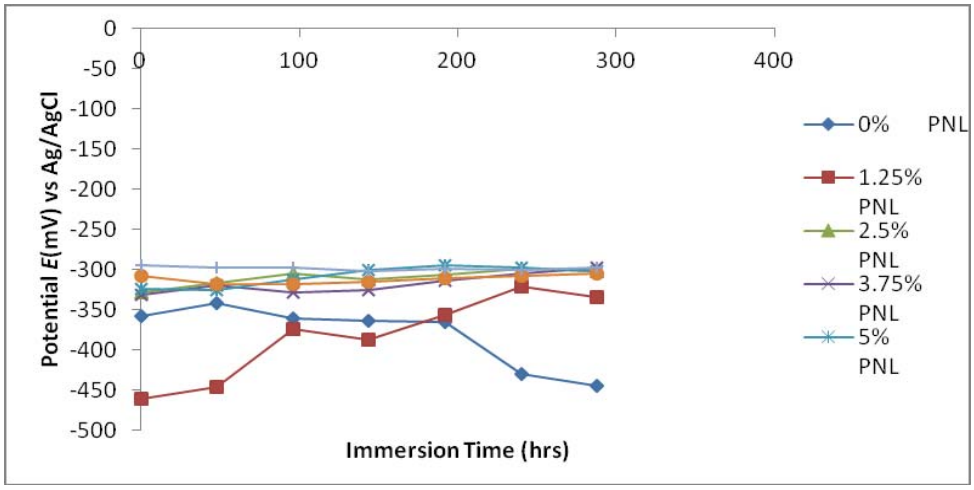

Fig. 6. Variation of potential with immersion time for potential measurements in 3 M H_2SO_4

the inhibitive action of PNL at this concentration. The influence of PNL on the electrochemical process is minimal as the corrosion potential after 288 h of exposure remains in the domain of intermediate corrosion, i.e. the corrosion protection is slightly effective. After 1.25% PNL concentration, the increase in the number of PNL molecules at higher concentrations has a profound influence on the electrochemical corrosion behaviour of the steel and the electrolytic action of the corrosion species. The marked decrease in potential values is due to the instantaneous action of the cationic species of PNL which are strongly adsorbed through electrostatic attraction unto the steel surface wherewith it chemisorbs through charge transfer. The heterocyclic atom (nitrogen) and the amine functional group are responsible for the film forming characteristics of the inhibitor.

Table 3. Data obtained from polarization resistance measurements for austenitic stainless steel in 3 M H_2SO_4 in presence of PNL.

Sample	Inhibitor Conc. (%)	Corrosion rate (mm/yr)	η	R_p (Ω)	E_{cr}, Obs (V)	i_{cr} (A)	I_{cr} (A/cm²)	*bc* (V/dec)	*ba* (V/dec)
A	0	7.95	0	3.77	-0.322	1.77E-03	6.97E-04	0.034	0.028
B	1.25	2.13	73.2	12.13	0.328	4.73E-04	1.86E-04	0.033	0.022
C	2.5	1.08	86.5	13.62	-0.328	2.41E-04	9.49E-05	0.018	0.013
D	3.75	1.02	87.2	32.35	-0.326	2.27E-04	8.94E-05	0.057	0.024
E	5	1.11	85.9	40.03	-0.41	2.47E-04	9.72E-05	0.094	0.03
F	6.25	1.08	86.3	57.12	0.329	2.41E-04	9.49E-05	0.034	0.46
G	7.5	1.12	86.1	42.17	0.325	2.50E-04	9.84E-05	0.048	0.049

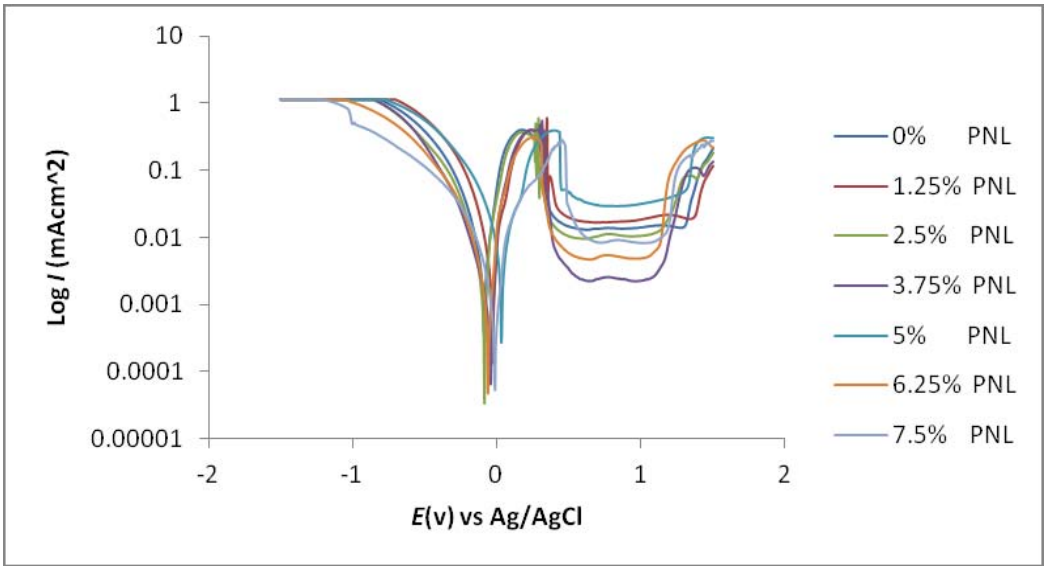

Fig. 7. Comparison plot of cathodic and anodic polarization scans for austenitic stainless steel in 3 M H_2SO_4 + 3.5% NaCl solution in the absence and presence of specific concentrations of PNL at 25°C (0% - 7.5% PNL)

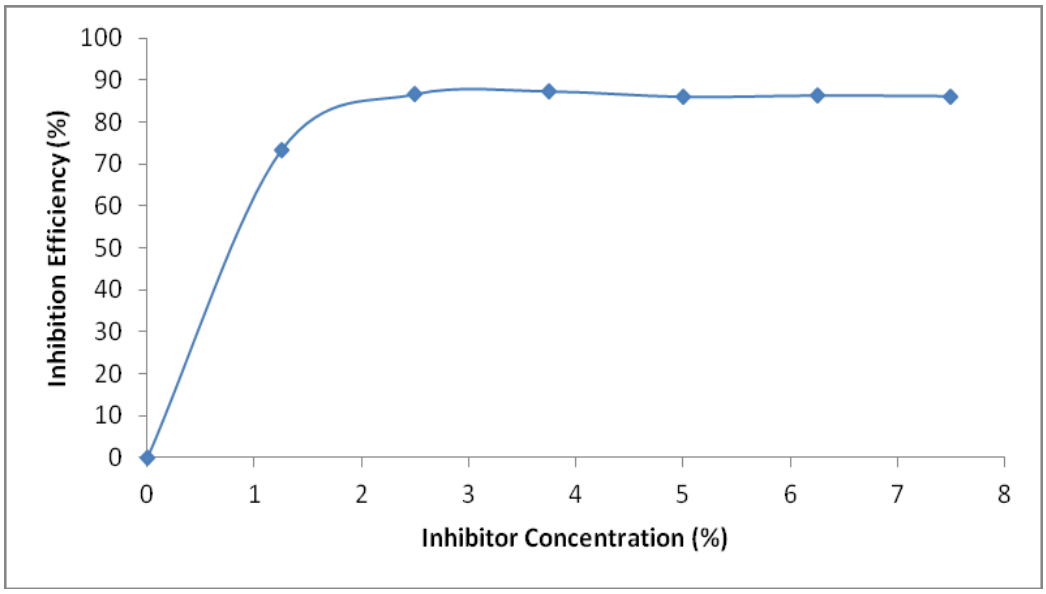

Fig. 8. Relationship between η and inhibitor concentration for polarization test in 3 M H_2SO_4

The protective film is responsible for the potential values after 1.25% PNL concentration (2.5% -7.5% PNL). The film prevents the diffusion of chlorides and sulphates responsible for anodic degradation of the steel in 0% PNL as observed in the corresponding potential values. The average potential at 288h after 1.25% PNL concentration ranges between ~300 and 302 mV which is well within the zone of passivation potentials for stainless steel. This is further confirmed from the corrosion rates and inhibition efficiency values. The intermolecular interaction resulting in the potential values obtained is explained under mechanism of inhibition.

Potentiodynamic polarization studies

Potentiostatic potential was cursorily examined from –1.50 to +1.50 V vs. Ag/AgCl at a scan rate of 0.0166 mV s^{-1}. The effect of the addition of PNL on the anodic and cathodic polarization curves of austenitic stainless steel type 304 in 3 M H_2SO_4 solutions at 25°C was studied at ambient temperature. Figure 7 shows the polarization curves of the stainless steel in absence and presence of PNL at specific concentrations in 3 M H_2SO_4, while figure 8 shows the variation of η versus inhibitor concentration. Results obtained using Tafel and linear polarization methods indicate that PNL inhibited the electrochemical process of corrosion. Anodic and cathodic currents were significantly influenced in the presence of PNL. The adsorption of PNL is slightly independent of the value of its concentrations as shown in figure 7; an average inhibition efficiency of 86% was maintained after 1.25% PNL.

Generally, all scans in figure 7 exhibited slightly similar behavior over the potential domain examined. The potential values alternates between the negative and noble values, an indication of its inhibitive impact on both the redox processes. The current density reduced sharply after 0% PNL concentration compared to all other PNL concentrations. The corrosion rate reduced drastically with differential variation in the electrochemical parameters. The inhibitive action of the PNL is related to its adsorption and formation of a barrier film on the electrode surface.

Electrochemical parameters such as, corrosion potential (E_{cr}), corrosion current (i_{cr}) corrosion current density (I_{cr}), cathodic Tafel constant (*bc*), anodic Tafel slope (*ba*) , surface coverage θ and percentage inhibition efficiency (η) were calculated and given in table 3. The corrosion current density (I_{cr}) and corrosion potential (E_{cr}) were determined by the intersection of the extrapolating anodic and cathodic Tafel lines, η was calculated from equation 6;

$$\eta = \frac{R_1 - R_2}{R_1}\% \qquad (6)$$

In table 3 PNL compound appeared to act as a mixed type inhibitor in 3 M H_2SO_4 since both cathodic and anodic reactions were influenced by the presence of PNL in the corrosive medium. Corrosion potentials slightly shifted in both directions in H_2SO_4, while the maximum displacement in E_{corr} value is 65 mV, thus PNL is a mixed type inhibitor but with greater tendency for anodic inhibition (Tao *et al*., 2009; Ferreira *et al*., 2004). PNL adsorption is influenced by the electronic properties of its functional groups (Cruz *et al*., 2004), i.e. the hydronium ion when it gains an electron and protonates in acid media. The results show that the mechanism of inhibition involves surface coverage of the steel sample by PNL molecules by physiochemical adsorption. PNL has an amino functional group (-NH_2), which protonates in the acid solution and becomes a hydronium ion (NH^+_3). The ionized PNL molecule dominantly competes with the hydrogen atom for electrons thus inhibiting hydrogen evolution reactions.

PNL can also be adsorbed over the metal surface in the form of neutral molecules. These molecules replace molecules of water on the metal surface and are electrostatically bonded to it through charge transfer. This in effect reduces the corrosion rate by blocking the sites available for anodic dissolution reactions. Chloride ions are first preabsorbed on the metal surface due to the dissociated atoms of iron in the solution. The process allows for the electrochemical diffusion of PNL cations onto the metal electrode as a result of the presence of the chloride ions which facilitates the adsorption electrostatically. The nitrogen atoms of the functional group are adsorbed on the surface inhibiting anodic reactions. Both processes enable the formation of coordinate bonds between PNL cations and the *d*-orbitals on the metal surface (Obot *et al*., 2012; Quraishi *et al*., 2007). The chemical adsorption type is probably the most important type of interaction between the metal surface and PNL molecule. PNL adsorbs on the metal surface due to interaction between the pi-electrons in its molecules and the metal d-orbitals via the chemisorption mechanism involving displacement of water molecules from the metal surface and the sharing of electrons between the two hetero atoms (nitrogen and oxygen) and the iron. Inhibition of the stainless steel corrosion by PNL was also found to depend on its electrochemical stability in the acidic media.

The micrograph (Fig. 9b) depict an irregular topography with micro hallows and perforations at high magnification. The micropits consist of sulphur and chloride atoms, thus proving the detrimental impact of these atoms on pit formation. They expedite the hydrolysis and electrolytic transport of charged iron atoms into the acid media after expulsing the preadsorbed oxygen ions. This phenomenon results in the rapid

degradation and corrosion of the alloy specimen, leading to the formation and growth of voids on the passive film. Eventually pit growth and dissolution of the alloy results. Individual pits are encompassed by a layer of iron oxide which partially envelopes the steel surface, confirming the formation of pits perpetually during the exposure hours while iron oxide forms over the surface.

Scanning electron Microscopy Analysis

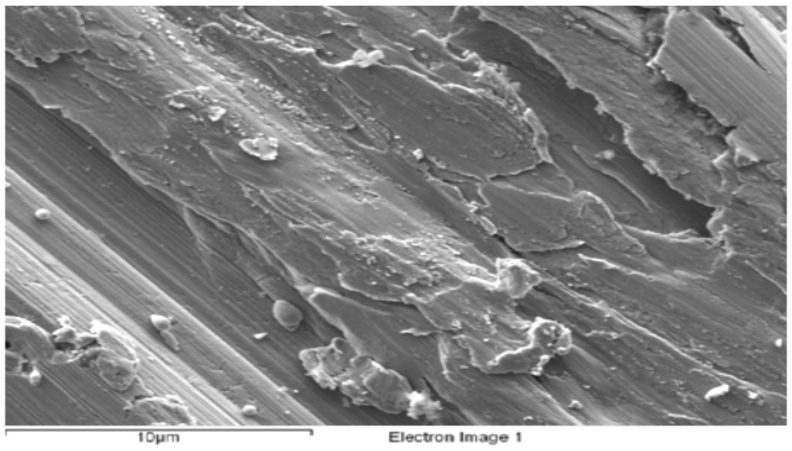

(a)

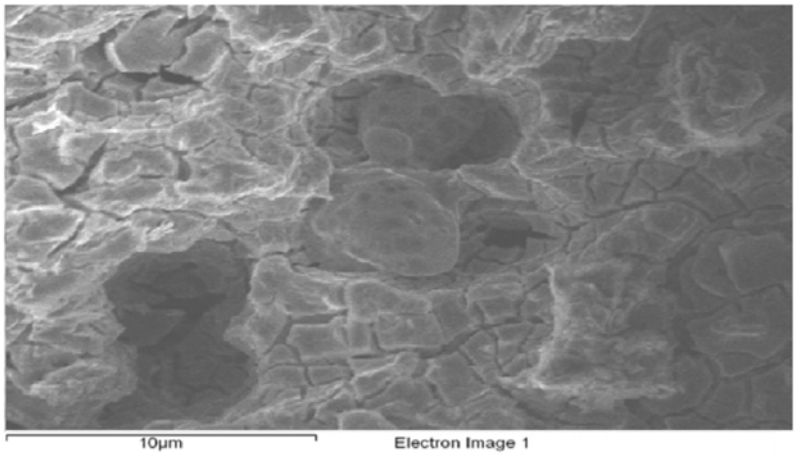

(b)

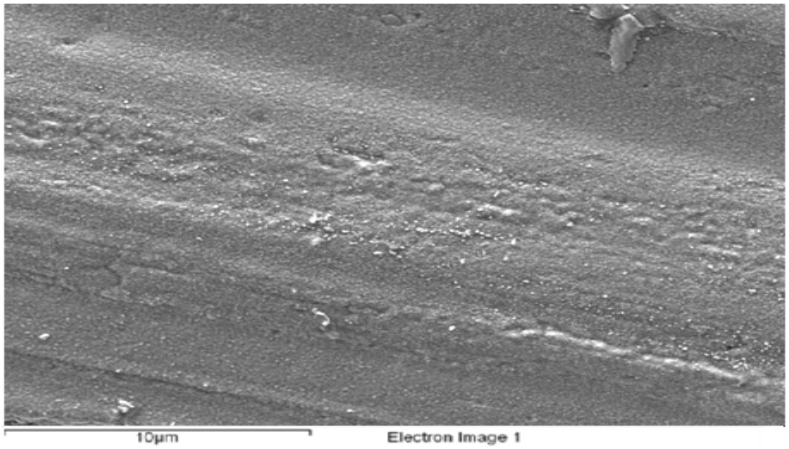

(c)

Fig. 9. SEM micrographs of: a) Austenitic stainless steel, b) Austenitic stainless steel in 3 M H_2SO_4, c) Austenitic stainless steel in 3 M H_2SO_4 with PNL.

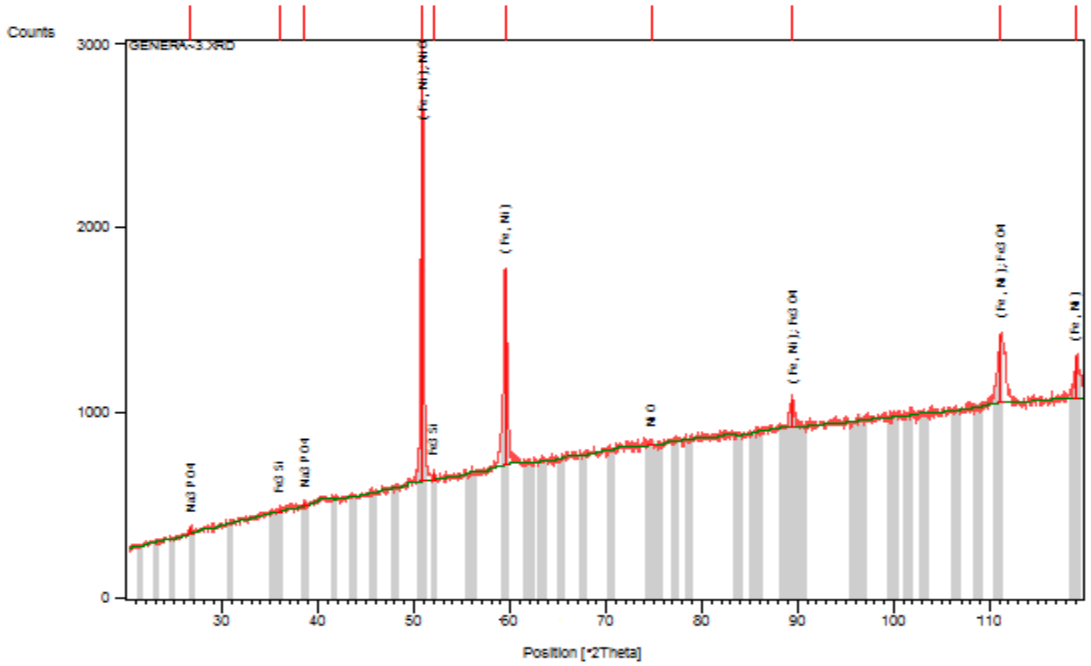

Fig. 10. XRD pattern of the surface film formed on austenitic stainless steel before immersion in the absence of PNL in 3 M H_2SO_4.

Table 4. Identified Patterns List for XRD analysis of austenitic stainless steel in 3 M H_2SO_4 without PNL.

Visible	Ref. Code	Score	Compound Name	Displacement [°2Th.]	Scale Factor	Chemical Formula
*	00-047-1417	61	Taenite, syn	-0.095	0.974	Fe , Ni
*	00-065-3005	41	Iron Silicon	-0.993	0.01	Fe_3 Si
*	00-008-0087	38	Iron Oxide	0.173	0.078	Fe_3 O_4
*	01-084-0195	25	Sodium Phosphate	-0.723	0.016	Na_3 PO_4
*	01-089-5881	21	Nickel Oxide	-0.018	0.341	Ni O

The improved morphology of the steel sample (Fig. 9c) is due to the crystalline precipitation of PNL molecules in the acid solution on the steel surface compared with the uninhibited sample. The strong adsorption of the molecules of PNL is most probably due to electrostatic attraction and electrochemical diffusion onto the surface of the steel whereby corrosive species are competitively displaced from the steel surface and simultaneously prevented from reaching the surface due to the protective barrier formed.

X-Ray Diffraction Analysis

X-ray diffraction (XRD) patterns of stainless steel surfaces from 3 M H_2SO_4 solutions are shown in figures 10 and 11, respectively. The identified patterns list for the XRD analysis of the steel in acid solution without PNL is shown in table 4. The peak values at 2θ values for the steel in the solution without PNL (Fig.10) showed the presence of iron oxides due to the redox corrosion process that took place on the steel surface. The electrochemical reaction resulted in the formation of the oxides as a result of the action of sulphate and chloride ion, responsible for the anodic dissolution process. The peaks at 2θ = 89.4° and 111.2° for the uninhibited steel in 3 M H_2SO_4 (Fig. 10) is attributed to iron (ii, iii) oxide (Fe_3O_4) while the peaks at 2θ = 39.5° and 50.5° can be assigned to iron (iii) oxide (Fe_2O_3). Observation of the diffraction peaks for the inhibited steel (Fig. 11) surfaces showed the absence of iron oxides and chemical compounds associated with corrosion. The compounds present especially chromium oxide at peak 2θ = 51° is responsible for the passivation of the steel in addition to the effective inhibiting action of PNL.

Adsorption isotherm

The mechanism of corrosion inhibition can be explained on the basis of the adsorption behaviour of the PNL on the metal surface. Adsorption isotherms are very important in determining the mechanism of organo - electrochemical reactions. It provides important clues to the nature of the metal-inhibitor interaction. For an inhibitor to have a high surface coverage on the metal, a

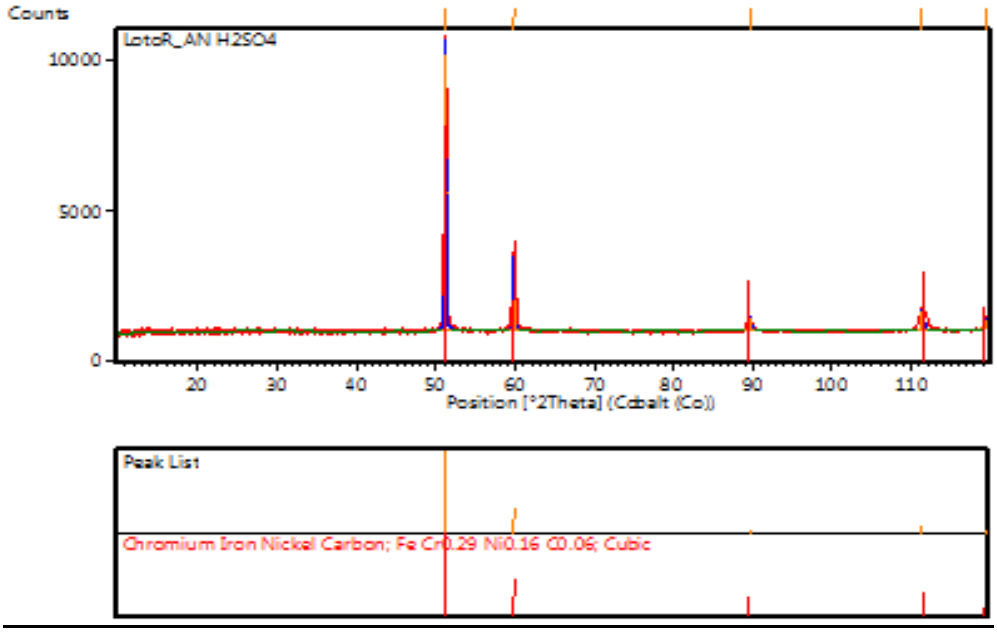

Fig. 11. XRD pattern of the surface film formed on austenitic stainless steel after immersion in the presence of PNL in 3 M H_2SO_4.

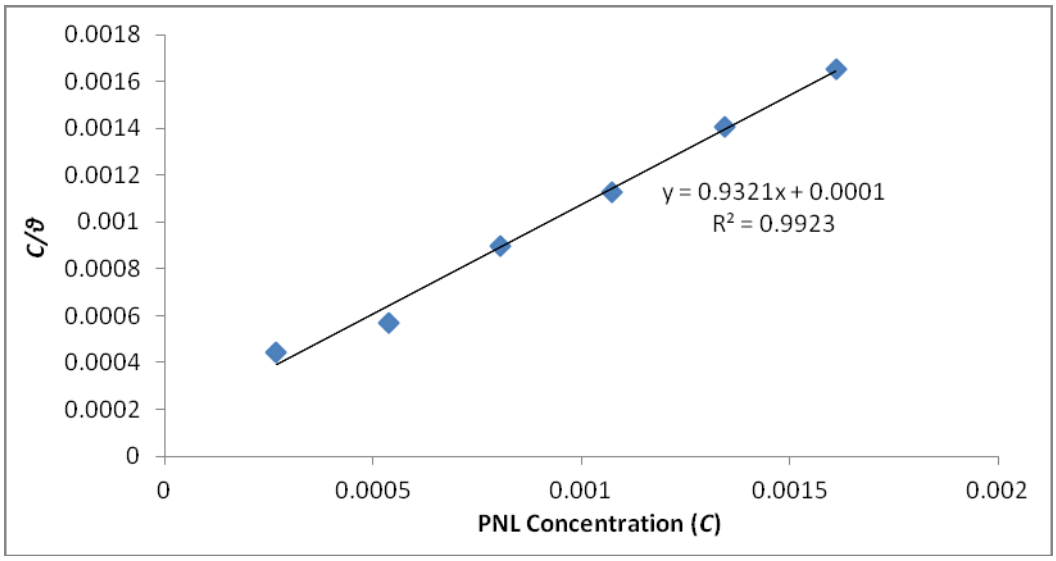

Fig. 12. Relationship between $\frac{C}{\theta}$ and inhibitor concentration (C) in 3 M H_2SO_4.

chemical bond between PNL molecule and the metal atom stronger than the one for water molecules/corrosive anions should be formed. The adsorption of corrosion inhibitors at the metal/solution interface is due to the formation of either electrostatic or covalent bonding between the adsorbate and the metal surface atoms. Langmuir adsorption isotherm was applied to describe the adsorption mechanism for the inhibiting compounds in acid solutions, as it best fit the experimental results.

The conventional form of the Langmuir isotherm is;

$$\left[\frac{\theta}{1-\theta}\right] = K_{ads}C \quad (7)$$

and rearranging gives

$$K_{ads}C = \left[\frac{\theta}{1+K_{ads}\theta}\right] \quad (8)$$

Table 5. Data obtained for the values of Gibbs free energy, surface coverage and equilibrium constant of adsorption at varying concentrations of PNL in 3 M H_2SO_4.

Inhibitor Concentration (C)	Free energy of Adsorption (ΔGads) (kJ/mol)	Surface Coverage (θ)	Equilibrium Constant of Adsorption (K_{ads})
0	0	0	0
0.000268	-31.33	0.601	5620.4
0.000537	-35.43	0.940	29187
0.000805	-33.04	0.900	11134
0.001074	-34.41	0.954	19209
0.001342	-33.90	0.954	15520
0.001611	-35.03	0.976	25075

θ is the extent of PNL coverage on the metal surface, C is the inhibitor concentration in the acid solution, and K_{ads} is the equilibrium constant of the adsorption. The graph of $\frac{C}{\theta}$ versus the inhibitor concentration C was depicts linearity (Fig.12) thus confirming Langmuir adsorption.

The deviation of the slopes from unity in figure 12 is attributed to the molecular interaction among the adsorbed inhibitor species on the metal surface and changes in the values of Gibbs free energy of adsorption with increasing surface coverage. This was not taken into consideration during the derivation of the Langmuir equation. Langmuir isotherm predicts unity as the value of the slope. However, the fitted line gave a value less than unity for the slopes. This suggests a slight deviation from ideal conditions assumed in Langmuir model.

Thermodynamics of the corrosion process

The values of the apparent free energy change i.e. Gibbs free energy (ΔG_{ads}) for the adsorption process can be evaluated from the equilibrium constant of adsorption using the following equation as shown in table 5.

$$\Delta G_{ads} = -2.303RT\log[55.5K_{ads}] \quad (9)$$

Where 55.5 is the molar concentration of water in the solution, R is the universal gas constant, T is the absolute temperature and K_{ads} is the equilibrium constant of adsorption. K_{ads} is related to surface coverage (θ) by the following equation.

$$K_{ads}C = \left[\frac{\theta}{1-\theta}\right] \quad (10)$$

The data in table 5 shows minimal difference from the ideal Langmuir model as observed in the results of Free energy of Adsorption (ΔG_{ads}) with increase in surface coverage (θ) values. The values of (ΔG_{ads}) for PNL depends surface coverage, this is due to the heterogeneous nature of the surface properties steel sample, thus the variation of the energy of adsorption as shown in table 5.

Results of ΔG_{ads} of about -20 kJ/mol are depicts with physisorption while values of -40 kJ/mol or above results in electrostatic interaction depicting chemisorptions (Obot *et al*., 2009; Hosseini *et al*., 2003). The calculated value of ΔG_{ads} is between −31.33 and −35.43 kJ mol^{-1} for PNL in sulphuric acid. The mechanism of adsorption of PNL on steel surface is physiochemical but tends to chemisorption. The intermolecular bonding is sufficiently strong to prevent displacement of adsorbed inhibitor molecules on the surface.

Statistical Analysis

Two-factor single level experimental ANOVA test (F - test) was used to analyze the separate and combined effects of the percentage concentrations of PNL and exposure time on the inhibition efficiency of PNL in the corrosion of inhibition of austenitic stainless steels in 3 M H_2SO_4 solutions and to investigate the statistical significance of the effects. The F - test was used to examine the amount of variation within each of the samples relative to the amount of variation between the samples.

The Sum of squares among columns (exposure time) was obtained with the following equations.

$$SS_c = \frac{\sum T_c^2}{nr} - \frac{T^2}{N} \quad (11)$$

Sum of Squares among rows (inhibitor concentration)

$$SS_r = \frac{\sum T_r^2}{nc} - \frac{T^2}{N} \quad (12)$$

Total Sum of Squares

$$SS_{Total} = \sum x^2 - \frac{T^2}{N} \quad (13)$$

The results using the ANOVA test is tabulated (Table 6) as shown.

Table 6. Analysis of variance (ANOVA) for inhibition efficiency of PNL inhibitor in 3 M H_2SO_4 (at 95% confidence level).

Source of Variation	Sum of Squares	Degree of Freedom	Mean Square	Mean Square Ratio	Min. MSR at 95% confidence Significance F	F%
Inhibitor concentration	7350.96	5	1470.19	145.16	2.71	95.75
Exposure Time	92.08	4	23.02	2.27	2.87	0
Residual	202.56	20	10.13			
Total	7645.60	29				

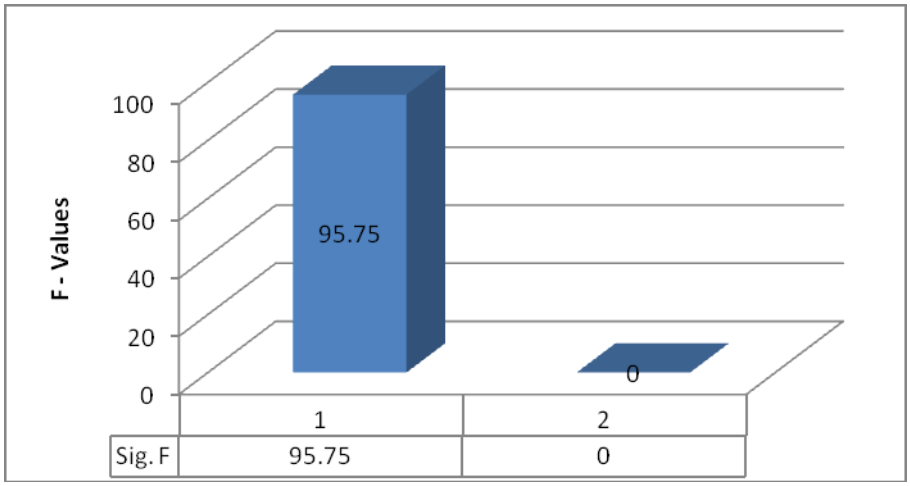

Fig. 13. Influence of inhibitor concentration and exposure time on inhibition efficiency in 3 M H_2SO_4.

The analysis in 3 M H_2SO_4 was evaluated for a confidence level of 95% i.e. a significance level of α = 0.05. The ANOVA results in the acid solutions reveal only one of the experimental sources of variation (inhibitor concentration) to be statistically significant on the inhibition efficiency with F -values of 145.16 in H_2SO_4. These are greater than significance factor at α = 0.05 (level of significance or probability). The F - values of exposure time in the solutions are less than the significant value factor hence they are statistically irrelevant. The statistical influence of the inhibitor concentration in H_2SO_4 (Fig. 13) is 95.75%. The influence of the exposure time is less than 0% thus practically negligible. The inhibitor concentration is the only significant model terms influencing inhibition efficiency of PNL on the corrosion of the steel specimen in the acid solutions. On this basis only percentage concentration of PNL significantly affects the inhibition efficiency of PNL in the acid media irrespective of the exposure time.

CONCLUSION

Aminobenzene performed effectively as a corrosion inhibiting compound, effectively reducing the corrosion rate of austenitic stainless steel at all concentrations studied from weight-loss, potential measurement and potentiodynamic polarization tests. The inhibition efficiency increased in direct proportion to increase in inhibitor concentration due to the availability of more inhibitor molecules to inhibit corrosion until saturation point. Adsorption of aminobenzene on the stainless steel obeyed Langmuir's adsorption isotherm, producing the best fit, thereby indicating that the molecular interaction is fixed and the effect of lateral interaction among the adsorbates on the value of Gibbs free energy is negligible. XRD analysis of the steel specimen surface showed diffraction peaks for the inhibited steel surfaces revealing the absence of iron oxides and chemical compounds associated with corrosion. At a confidence level of 95% the ANOVA results in test solutions showed only the inhibitor concentrations to be statistically significant on the inhibition efficiency of aminobenzene.

REFERENCES

Akrout, H., Maximovitch, S., Bousselmi, L., Triki, E. and Dalard, F. 2007. Evaluation of corrosion non toxic inhibitor adsorption for steel in near neutral solution: L(+) ascorbic acid. Materials Corrosion. 58:202-6.

Bera, S., Rangarajan, S. and Narasimhan, SV. 2000. Electrochemical passivation of iron alloys and the film characterisation by XPS. Corrosion Science. 42:1709 -24.

Bhaskaran, R., Palaniswamy, N., Rengaswamy, NS. and Jayachandran, M. 2003. ASM Handbook. (vol. 13A Corrosion): Fundamentals, Testing, and Protection, ASM International, New York, USA. 13B:621.

Bouklah, M., Ouassini, A., Hammouti, B. and El Idrissi, A. 2006. Corrosion inhibition of steel in sulphuric acid by pyrrolidine derivatives. Applied Surface Science. 252:2178-185.

Bouklah, M., Ouassini, A., Hammouti, B. and El Idrissi, A. 2006. Corrosion inhibition of steel in sulphuric acid by pyrrolidine derivatives. Applied Surface Science. 252:2178-85.

Chetouani, A., Medjahed, K., Sid-Lakhdar, KE., Hammouti, B., Benkaddour, M. and Mansri, A. 2004. Poly(4-vinylpyridine-poly(3-oxide-ethylene) tosyle) as an inhibitor for iron in sulphuric acid at 80°C. Corrosion Science. 46:2421-30.

Cruz, J., Martínez, R., Genesca, J. and García-Ochoa, E. 2004. Experimental and theoretical study of 1-(2-ethylamino)-2-methylimidazoline as an inhibitor of carbon steel corrosion in acid media. Journal of Electroanalytical Chemistry. 566(1):111-21.

Dadgarnezhad, A., Sheikhshoaie, I. and Baghaei, F. 2004. Corrosion inhibitory effects of a new synthetic symmetrical Schiff-base on carbon steel in acid media. Anti-Corrosion Method and Material. 51:266-71.

Deflorian, F. and Rossi, S. 2006. An EIS study of ion diffusion through organic coatings. Electrochimical Acta. 51:1736-44.

Ferreira, ES., Giacomelli, C., Giacomelli, FC. and Spinelli, A. 2004. Evaluation of the inhibitor effect of L-ascorbic acid on the corrosion of mild steel. Materials Chemistry and Physics. 83: 29-143.

Ferreira, ES., Giacomelli. CF., Gicomelli, FC. and Spinelli, A. 2004. Evaluation of the inhibitor effect of l-ascorbic acid on the corrosion of mild steel. Materials Chemistry and Physics. 83: 129-134.

Gopi, D., Bhuvaneswaran, N., Rajeswar, IS. and Ramadas, K. 2000. Synergistic effect of thiourea derivatives and non ionic surfactants on the inhibition of corrosion of mild steel in acid environment. Anti-Corrosion Methods and Materials. 47:332-38.

Gopi, D., Manimozhi, SKM., Govindaraju, KM., Manisankar P. and Rajeswari, S. 2007. Surface and electrochemical characterization of pitting corrosion behaviour of 304 stainless steel in ground water media. Journal of Applied Electrochemistry. 37:439-49.

Hosseini, MG., Mertens, SFL. and Arshadi, MR. 2003. Synergism and antagonism in mild steel corrosion inhibition by sodium dodecylbenzenesulphonate and hexamethylenetetramine. Corrosion Science. 45:1473-89.

Hosseini, SMA., Salari, M. and Ghasemi, M. 2009. 1-Methyl-3-pyridine-2-yl-thiourea as inhibitor for acid corrosion of stainless steel. Materials Corrosion. 60:963-68.

Kane, RD. 2003. ASM Handbook. (vol. 13A Corrosion): Fundamentals, Testing, and Protection. ASM International, New York, USA. 13:922.

Martin, RL. 2003. Corrosion Inhibitors for Oil and Gas Production in ASM Handbook. (vol. 13A Corrosion): Fundamentals, Testing, and Protection. ASM International, New York, USA. 13: 878-886.

Mieczyslaw, S. and Joanna, T. 2013. Adenine as an Effective Corrosion Inhibitor for Stainless Steel in Chloride Solution. International Journal of Electrochemical Science. 8:9201-21.

Negm, NA. and Aiad, IAJ. 2007. Synthesis and Characterization of Multifunctional Surfactants in Oil-Field Protection Applications. J. Surf. Deterg. 10:87-92.

Negm, NA. and Mohamed, AS. 2004. Surface and thermodynamicproperties of diquaternary bola-form amphiphiles containingaromatic spacer. Journal of Surfactants and Detergents. 7:23-30.

Noor, EA. 2005. The inhibition of mild steel corrosion in phosphoric acid solutions by some N-heterocyclic compounds in the salt form. Corrosion Science. 47:33-55.

Obot, IB., Ebenso, EE., Obi-Egbedi, NO., Ayo, SA. and Zuhair, MG. 2012. Experimental and theoretical investigations of adsorption characteristics of itraconazole as green corrosion inhibitor at a mild steel/hydrochloric acid interface. Research in Chemical Intermediates. 38:1761-71.

Obot, IB., Obi-Egbedi, NO. and Odozi, NW. 2010. Acenaphtho [1,2-b] quinoxaline as a novel corrosion inhibitor for mild steel in 0.5 M H_2SO_4. Corrosion Science. 52:923-26.

Obot, IB., Obi-Egbedi, NO. and Umoren, SA. 2009. Experimental and theoretical investigation of clotrimazole as corrosion inhibitor for aluminium in hydrochloric acid and effect of iodide ion addition. Der Pharma Chemica. 1:151-66.

Olsson, COA. and Landolt, D. 2000. Passive films on stainless steels chemistry, structure and growth. Electrochimical Acta. 48:1093-104.

Popova, A., Sokolova, E., Raicheva, S. and Christov, M. 2003. AC and DC study of the temperature effect on mild steel corrosion in acid media in the presence of benzimidazole derivatives. Corrosion Science. 45:33-58.

Quraishi, MA., Rafiquee, MZA., Khan, S. and Saxena, N. 2007. Corrosion inhibition of aluminium in acid solutions by some imidazoline derivatives. Journal of Applied Electrochemistry. 37:1153-62.

Satapathy, A., Gunasekaran, KG., Sahoo, SC., Kumar, A. and Rodrigues, PV. 2009. Corrosion inhibition by *Justicia gendarussa* plant extract in hydrochloric acid solution. Corrosion Science. 51:2848-56.

Selvakumar, P., Balanaga, BK. and Thangavelu, C. 2013. Corrosion inhibition study of Stainless steel in Acidic medium – An Overview. Research Journal of Chemical Sciences. 3(4):87-95.

Sk, A., Ali, MT., Saeed. and Rahman, SU. 2003. The isoxazolidines: a new class of corrosion inhibitors of mild steel in acidic medium. Corrosion Science. 45:253-66.

Tao, ZH., Zhang, ST., Li, WH. and Hou, BR. 2009. Corrosion inhibition of mild steel in acidic solution by some oxo-triazole derivatives. Corrosion Science. 51:2588-95.

Taveira, LV., Frank, G., Strunk, HP. and Dick, LFP. 2005. The influence of surface treatments in hot acid solutions on the corrosion resistance and oxide structure of stainless steels. Corrosion Science. 47:757-69.

Trabanelli, G. 1991. Inhibitors-an old remedy for a new challenge. Corrosion. 47:410-19.

Wojtanowicz, AK. 2008. Environmental technology in the oil industry, Springer, Berlin 17:51.

Received: Sept 25, 2014; Revised: Nov 6, 2014; Accepted: Feb 3, 2015